Chaotic and regular trajectories in the Antarctic Circumpolar Current

By JONAS NYCANDER[1,2]*, KRISTOFER DÖÖS[1] and ANDREW C. COWARD[3], [1]*Meteorologiska institutionen Stockholms universiteit, S-106 91 Stockholm, Sweden*; [2]*Defence Research Establishment, S-172 90 Stockholm, Sweden*; [3]*Southampton Oceanography Centre, Southampton SO14 3ZH, UK*

(Manuscript received 11 October 2000; in final form 30 May 2001)

ABSTRACT

Methods from chaos theory are applied to the analysis of the circulation in the Southern Ocean, using velocity fields produced by a realistic global ocean model. We plot the intersections of individual trajectories encircling Antarctica with a vertical plane in the Drake passage. This so-called Poincaré section shows a drastic difference between regular trajectories in a core region of the Antarctic Circumpolar Current (ACC), and chaotic, mixing trajectories in the surrounding region. It also shows that there is a region with overturning circulation of approximately 3.5 Sv in the ACC, with downwelling on the northern side and upwelling on the southern side, which may be related to the Deacon cell.

1. Introduction

One of the main products of model simulations of the global ocean circulation is the time-averaged, three-dimensional (3D) velocity field. However, it is a nontrivial task to visualise and understand the qualitative properties of this field.

For a corresponding two-dimensional (2D) stationary velocity field, there are no such difficulties; all that is needed is to show a contour plot of the stream function (given that the velocity field is incompressible). All fluid particles follow these contours, and there is no mixing across them.

The traditional way to look at the 3D circulation is to integrate the velocity field over one of the spatial coordinates. Thus, by integration over depth one obtains the barotropic stream function, and by zonal integration the meridional stream function. Superficially, they resemble the stream function of a 2D flow; however, these integrated stream functions in fact reveal little of the proper-

ties of the real streamlines. They also give a false impression of the regularity of the flow. Indeed, a stationary 3D velocity field is in general mixing, and a single trajectory space-filling.

A notable illustration of the difficulties is the Deacon cell, a large overturning cell of magnitude 15–20 Sv in the zonally integrated meridional stream function in global ocean models, situated between approximately 40°S and 60°S. The Deacon cell has puzzled oceanographers, since it has been difficult to identify the corresponding 3D circulation pattern (Hirst et al., 1996).

In principle, such an overturning cell might correspond to many different types of circulation. One hypothesis is that the Deacon cell is the result of the variable depth of the isopycnic surfaces (Döös and Webb, 1994; Döös, 1994). If such a surface is deeper where the flow along it is southward than where it is northward, zonal integration will result in an overturning cell like the Deacon cell. This is true even if the fluid particles always stay on the same isopycnic surface, so that there is actually no overturning circulation in the usual sense.

---

* Corresponding author.
e-mail: jonas@misu.su.se

The mathematical properties of stationary 3D flows are very similar to those of time-periodic 2D flows. Simple model flows of both kinds have long been studied in chaos theory (Beloshapkin et al., 1989; Polvani and Wisdom, 1990; Pierrehumbert, 1991; Behringer et al., 1991; Fountain et al., 1998). The standard tool used in these studies is called Poincaré section. In the case of a stationary 3D flow, this is a plot of successive intersections of a particle trajectory with a fixed surface. We will use this technique here to study particle trajectories in the Antarctic Circumpolar Current (ACC), which flows eastward around Antarctica. It is the Earth's strongest ocean current, with a magnitude of 130 Sv, and dominates the circulation in the Southern Ocean.

We find that the basic structure of the flow is similar to what has previously been seen in simple model flows, although the flow studied here is vastly more complex. In particular, the Poincaré section shows a drastic difference between regular trajectories in a core region of the ACC, and chaotic, mixing trajectories in the surrounding region. It also shows that there is a region with overturning circulation of approximately 3.5 Sv in the ACC, with downwelling on the northern side and upwelling on the southern side.

2. Regular and chaotic trajectories

The particle trajectories studied in this paper have been calculated using the time-averaged velocity field from the last four years of a twelve-year simulation with the global model OCCAM (Webb, 1996, 2000). This model has 36 vertical levels and a horizontal resolution of $0.25°$.

In Fig. 1 we show 32 particle trajectories that start in or near the ACC. Each one has been continued 30 circuits around Antarctica, or until it leaves the Southern Ocean.

Figure 2 is a Poincaré section showing the intersections of these trajectories with a vertical plane at $70°W$, i.e. in the Drake Passage. Sixteen of the trajectories (the red dots) start slightly north of the core region of the ACC. They quickly spread, half of them leaving the Southern Ocean before completing 10 circuits, and the rest before completing 27 circuits.

The remaining 16 trajectories (in blue) start in the core of the ACC, spaced in the same way as the starting points of the red trajectories. For a long time they are trapped in the ACC, returning almost to the same position each time after encircling Antarctica. The first trajectory escapes after 17 circuits, and all except three remain in the core region after 30 circuits.

A similar drastic difference between the mixing behaviour in different regions has been seen in numerous studies of chaotic advection in simple Hamiltonian systems (Lichtenberg and Lieberman, 1983; Beloshapkin et al., 1989; Polvani and Wisdom, 1990; Pierrehumbert, 1991). It is there a result of the existence of invariant "KAM tori", corresponding to invariant curves on the Poincaré section, i.e. curves that are mapped onto themselves. (The trajectories define a mapping on the Poincaré section, each point being mapped onto the point where the trajectory going through it intersects the Poincaré section the next time.) The existence of such KAM tori is proved by the KAM (Kolmogorov–Arnold–Moser) theorem, provided that the mapping satisfies the appropriate conditions (Lichtenberg and Lieberman, 1983).

A KAM torus is a perfect barrier to transport: no trajectory inside can ever get out, and vice versa. Trajectories inside a KAM torus are in general regular, while those outside the outermost KAM torus are chaotic, and diverge exponentially.

The magnified Poincaré section in Fig. 3 shows another set of trajectories. The four ones in the trapped region may seem to lie on invariant curves, suggesting the existence of KAM tori. However, this is not quite true, and if these trajectories are continued, they eventually escape from the ACC.

Two conditions are essential for the KAM theorem to hold. First, the mapping should be area preserving, i.e. any closed curve should be mapped onto a closed curve with equal enclosed area. In our case this condition holds in a modified form, since the mapping preserves the measure $u \, dS$, i.e. it is area preserving with the zonal velocity u as normalisation constant. (This follows from mass conservation along any flux tube bounded by trajectories.) As long as u is nonzero and does not change sign, this modification of the area preservation does not essentially change the properties of the mapping. In the part of Drake passage that we study, u is positive everywhere.

The second condition of the KAM theorem is that the mapping is continuously differentiable a
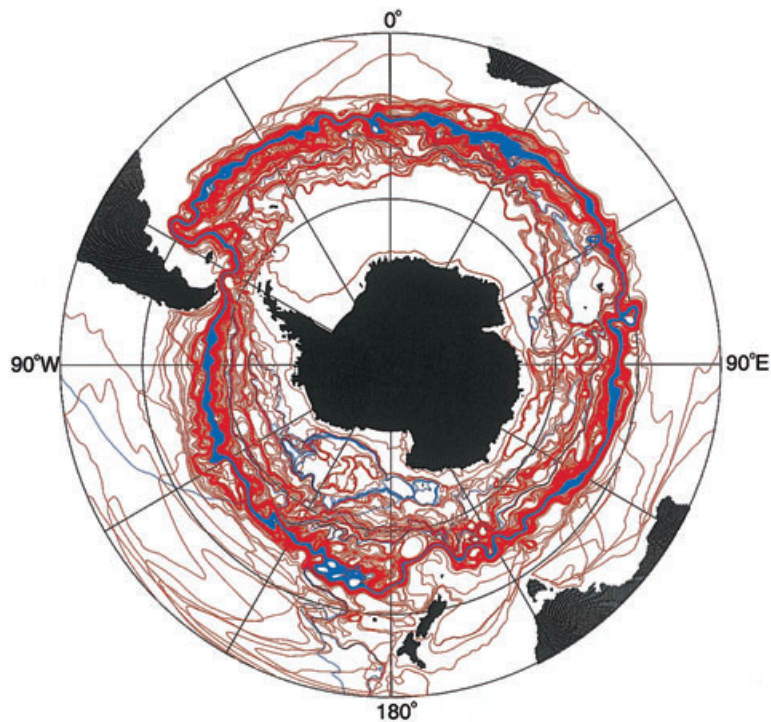
Fig. 1. Thirty-two particle trajectories in the Southern Ocean, each one encircling Antarctica several times. The 16 blue trajectories start in the core of the ACC, and the 16 red ones slightly outside.

sufficient number of times, so that, for example, a smooth closed curve is mapped onto another smooth closed curve (Lichtenberg and Lieberman, 1983). This is not quite true in our case, because of the interpolation scheme used to define the velocity field inside each grid cell. Each velocity component was taken to be constant in the transverse directions, and interpolated linearly in the parallel direction (Döös, 1995; Blanke and Raynaud, 1997). (For example, inside each grid cell the zonal component u is a linear function of only the longitude.) This simple scheme was used because it is exactly mass conserving, and because it allows a very fast algorithm to be used when calculating the trajectories.

Hence, the interpolated velocity field has tangential discontinuities on the faces between grid cells. In general the discontinuities are small, but they nevertheless change the properties of the mapping, and the KAM theorem is not valid. Simply speaking, the effect of such discontinuities is that the KAM tori become "fuzzy", and are no

longer perfect barriers to transport. However, if the discontinuities are small, the "fuzzy KAM tori" (which are in fact not KAM tori) still trap the trajectories inside them for a very long time. We have observed this effect in simulations of simple analytically defined mappings with a discontinuity, and the same thing occurs here.

Thus, the "fuzziness" of the KAM tori is a numerical artifact, and from an oceanographic point of view it is not essential. The important point is the contrast between the regular core region, bounded by a "fuzzy KAM torus", where the trajectories are trapped during dozens of circuits around Antarctica, and the outer stochastic region where they mix and disperse. This structure, seen in Fig. 2, is quite similar to that seen many times in simple model flows.

3. Overturning circulation

Traditionally, the global overturning circulation is studied by computing the meridional stream
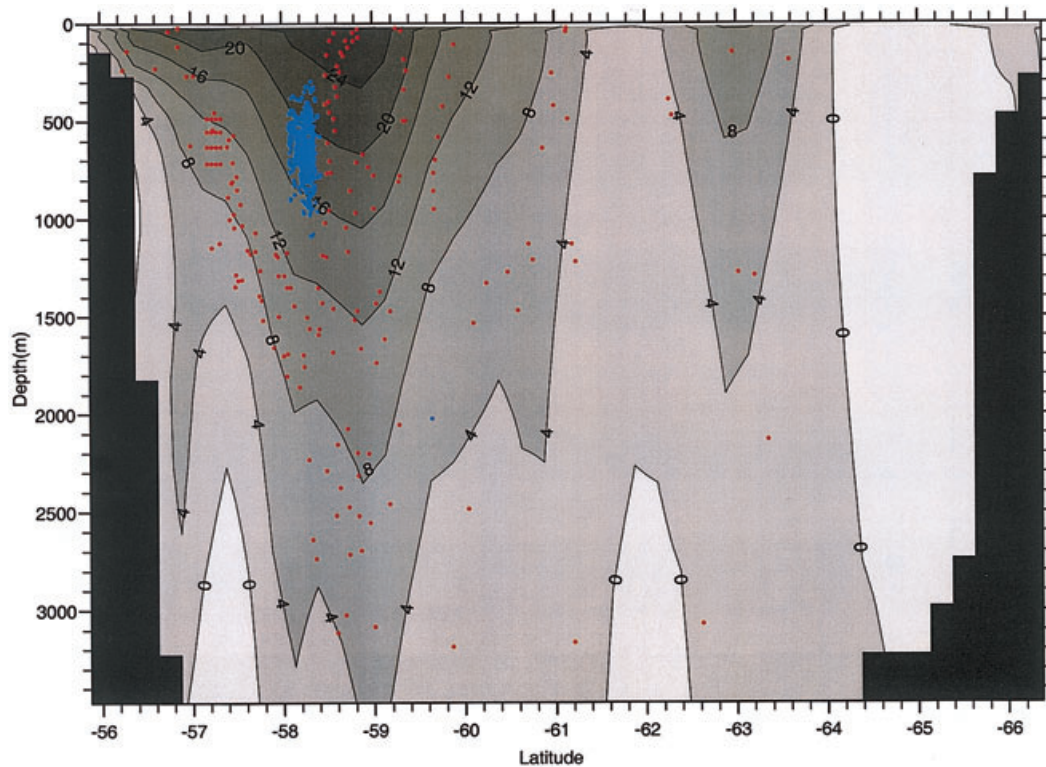
Fig. 2. Poincaré section in the Drake Passage, showing the intersections of the trajectories in Fig. 1 (with the same colours) with a vertical plane at 70°W. Only intersections from west to east are shown. The contours indicate the zonal velocity u in cm s^{-1}. The starting points of the red trajectories were regularly spaced in a small rectangle at 57.2°S and 500–700 m depth. The blue trajectories started in a similar rectangle at 58.2°S.

function by zonal integration of the velocity field. In Fig. 4 we show the meridional stream function obtained from the same velocity field as used in the trajectory calculations in Figs. 1–3. The dominant feature in the Southern Ocean is the Deacon cell, the large overturning cell between 38°S and 61°S, with an amplitude of 20 Sv.

We will now define an analogue of the meridional stream function on the Poincaré section. On KAM tori, this can be done rigorously. As shown in Fig. 5, the meridional flow between two KAM tori is equal to the integral $\int_A u \, dS$, where A is a surface bounded by the KAM tori and by two successive iterations of a line connecting them. Thus, this integral gives the difference $\Delta\psi$ between the value of the stream function ψ on the two KAM tori. The invariance property of the mapping guarantees that this definition is unique. Since no trajectories can cross the KAM tori, it is

entirely legitimate to think of the invariant curves (i.e. the intersections between the KAM tori and the Poincaré section) as streamlines on the Poincaré section.

We emphasise the principal difference between this stream function, and the traditional zonally integrated meridional stream function. The latter tells very little about the 3D structure of the trajectories; for example, an overturning cell might be the result of a zonal average over many small and disconnected overturning cells, or of circulation along sloping isopycnic surfaces (Döös and Webb, 1994; Döös, 1994). The stream function defined on KAM tori, on the other hand, directly reflects the 3D structure of the trajectories.

Away from the KAM tori a stream function cannot be rigorously defined. The basic problem is that the trajectories mix, and hence some trajectories would cross whatever curves were chosen as
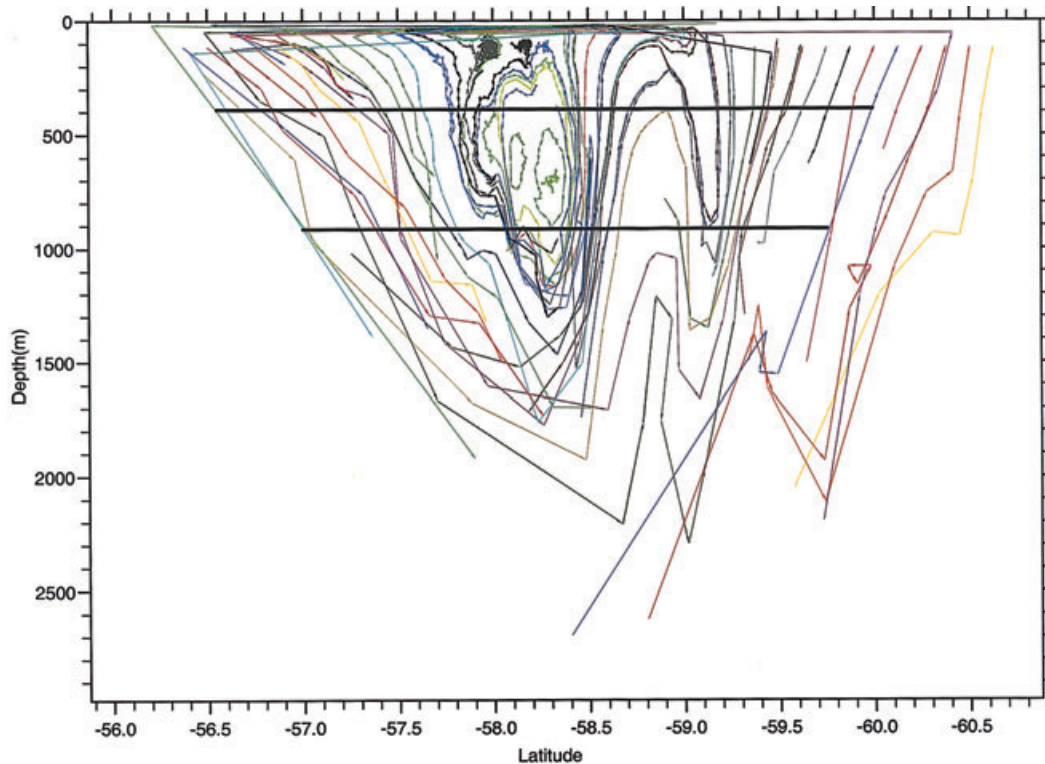
Fig. 3. Magnified Poincaré section in the Drake passage. Successive intersections of the same trajectory have here been connected by arrows. The starting points are regularly spaced along a horizontal line at 138 m depth, and the trajectories have been followed forward and backward until they enter the strongly irregular region or leave the Southern Ocean. Four additional trajectories have been selected to display the flow in the regular core region, which is entirely below 138 m. (They are not the same as any of the blue trajectories in Fig. 2, but they are in the same region.) The meridional transport across the thick horizontal lines has been calculated numerically.

streamlines. However, if the displacement δr of a trajectory after one circuit is small, the flow is almost regular. This is the case in the ACC, as seen in Fig. 3, where successive displacements δr of each trajectory are shown. The resulting curves may be thought of as "approximate streamlines", since most displacements are approximately parallel locally. We see that there is downwelling on the northern side between 56.5°S and 58°S, and upwelling on the southern side between 58.5°S and 61°S (with a narrow downwelling region around 59°S).

In the region without any trajectories in Fig. 3 it makes no sense to think of a meridional flow on the Poincaré section. Here the displacements are large and erratic, and close trajectories often diverge strongly already after one circuit. In some

parts of this region many trajectories also leave the Southern Ocean before completing one circuit. The trajectories shown in Fig. 3 have been terminated when they enter into this strongly stochastic region, and when they diverge strongly from nearby trajectories. (There is a fair amount of small-scale noise in the displacement field δr, even in the regular region.)

The upwelling and downwelling regions are only partly connected. Many of the trajectories in the downwelling region enter into the deep layer below 2000 m, where the displacements are irregular and the zonal velocity u is small. Similarly, many of the upwelling trajectories originate in this deep layer. When the upwelling trajectories come close to the surface, they enter into the Ekman layer, and are rapidly swept northward. Most of
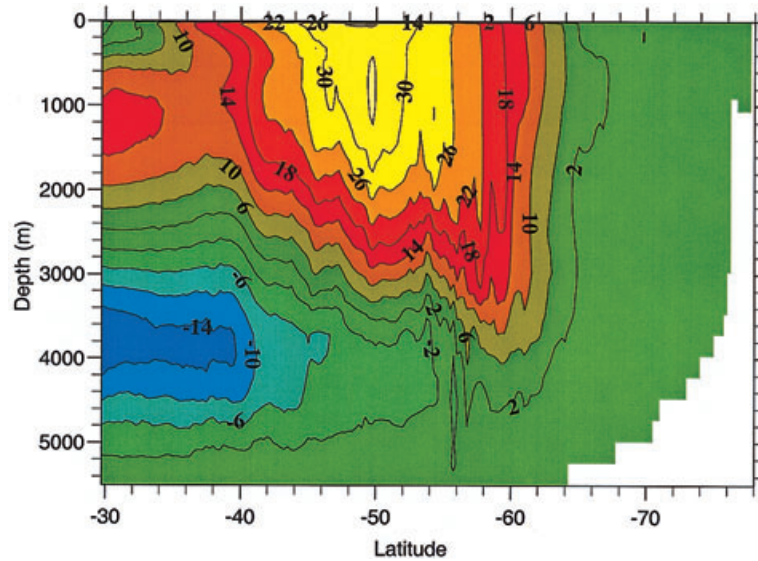
Fig. 4. The meridional stream function in the Southern Ocean as a function of depth and latitude. It has been obtained by zonal integration of the velocity field used in the trajectory calculations in Figs. 1–3. Units are in Sverdrups.
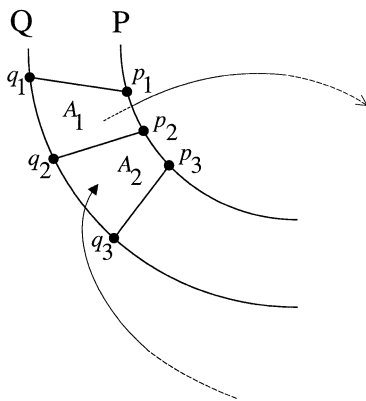
Fig. 5. Definition of stream function on a Poincaré section. *P* and *Q* are two KAM tori. The points p_1, p_2 and p_3 are successive intersections of one trajectory, q_1, q_2 and q_3, of another one. Thus, the region A_1 is mapped onto A_2 after one circuit, which takes the time *T*. The water flowing through A_1 during the time *T* can be considered as a meridional flow of the same amount of water across the line $q_2 - p_2$ during this time. The meridional mass flux between the KAM tori *P* and *Q* is therefore equal to the integral $\int_{A_1} u \, dS = \int_{A_2} u \, dS$.

these leave the Southern Ocean (they are then terminated in Fig. 3), but some of them enter into the downwelling region on the northern side of the ACC.

To estimate the magnitude of the meridional flow, we have calculated the integral $\int u \delta z \, dy$ along the horizontal thick lines at 389 m depth and 915 m depth in Fig. 3. Here δz is the depth displacement of a trajectory after one circuit. (This expression follows from the same argument as in Fig. 5, and is equivalent to regarding $\delta r/T$ as a meridional velocity; however, it should not be forgotten that strictly speaking there is no continuous meridional flow, only discrete displacements.) The numerical integration step was $0.0025°$, i.e. 400 trajectories per degree were used. We find that the downwelling across the thick lines north of $58.25°$S is 3.5 ± 0.5 Sv, while the upwelling south of $58.25°$S is 3.3 ± 0.5 Sv. (The error bounds were estimated by comparing the results from the two different depths, and also by comparing the results when following the trajectories one circuit backward and forward from a given depth, respectively.)

Figure 3 should be compared with the tradi-

tional zonally integrated meridional stream function in Fig. 4, which is dominated by the Deacon cell. The nature of this overturning cell has been controversial since it has been difficult to identify the corresponding 3D circulation pattern (Hirst et al., 1996).

The meridional flow seen in Fig. 3 is reminiscent of the Deacon cell, but here there are no difficulties of interpretation. We have precisely identified the trajectories that are responsible for the up- and downwelling, while spiralling around Antarctica. This is true overturning circulation, which cannot be an artificial result of zonal integration. We have not investigated the nature of the implied diapycnal flow (in principle, it could also be a result of remaining model drift during the last four years of the OCCAM integration).

The magnitude of the meridional circulation in Fig. 3 is less than 20% of the magnitude of the Deacon cell. There are at least two possible explanations for this. The first is that there may be additional up- and downwelling in other parts of the Southern Ocean, where the trajectories do not encircle Antarctica many times; this would not show up in Fig. 3. The second, already mentioned explanation is that much of the Deacon cell is caused by circulation along sloping isopycnals. This is supported by the fact that a large part of the overturning circulation vanishes if the integration is done along isopycnals instead of depth levels, as shown by Döös and Webb (1994) and by Döös (1994).

The width of the region with meridional circulation seen in Fig. 3 is less than 4°, which is much narrower than the Deacon cell. However, since the cross-sectional area is inversely proportional to the zonal velocity u, the structure seen in Fig. 3 is broader in other places than in the Drake passage. It is also interesting to note that because of the north–south displacements of the ACC seen in Fig. 1, a zonal average would result in a width comparable to the Deacon cell.

4. Discussion and conclusion

In this paper we have introduced a new method of analysing and visualising the 3D structure of the steady ocean circulation. This method has long been used in chaos theory, and consists of plotting successive intersections of individual tra-

jectories with given vertical surface, a so-called Poincaré section.

The traditional way of analysing the overturning circulation is to integrate the velocity zonally, along curves with fixed depth and latitude. This eliminates the horizontal gyre circulation. However, the ocean circulation has a tendency to follow the isopycnals rather than being on fixed depths, and if the isopycnal surfaces slope, the gyre also has a vertical component. Therefore an integration along isopycnals eliminates a larger part of the gyre circulation (Döös and Webb, 1994; Döös, 1994; Hirst et al., 1996). The successive displacements on a Poincaré section are in effect a result of an integration along the trajectories. This eliminates all the gyre circulation, leaving only the true overturning circulation.

By plotting particle trajectories in the ACC on a Poincaré section we have revealed features of the 3D structure of the ocean circulation that cannot be seen on the traditional zonally integrated meridional stream function. In particular, we have seen that the trajectories in a core region of the ACC are regular and almost trapped there, while the trajectories in the surrounding region are chaotic and mixing. This structure is similar to what has previously been seen in simple model flows, although the flow studied here is vastly more complex. Perhaps there is a connection to the fact that the concentration of dissolved oxygen in hydrographic sections has a minimum in the ACC, indicating that this water is old (Hoppema et al., 2000).

We have also revealed the existence of a region with overturning circulation of approximately 3.5 Sv in the ACC, with downwelling on the northern side and upwelling on the southern side. This overturning occurs in the region where the trajectories encircle Antarctica many times. There may well exist additional overturning in other parts of the Southern Ocean.

The velocity field we use is time-averaged, and an important question is how time-dependent fluctuations would affect the results. Preliminary calculations with seasonal fluctuations included in the velocity field indicate that at least the up- and downwelling found here is not affected very strongly. However, further work is needed to investigate whether the core region with trapped fluid survives the fluctuations. In any case, averaging over only one coordinate (i.e. time) is an

important step forward compared to averaging over two coordinates (i.e. time and longitude), as is done traditionally.

REFERENCES

Behringer, R. P., Meyers, S. D. and Swinney, H. L. 1991. Chaos and mixing in a geostrophic flow. *Phys. Fluids A* **3**, 1243–1249.

Beloshapkin, V. V., Chernikov, A. A., Natenzon, M. Ya., Petrovichev, B. A., Zagdeev, R. Z. and Zaslavsky, G. M. 1989. Chaotic streamlines in pre-turbulent states. *Nature* **337**, 133–137.

Blanke, B. and Raynaud, S. 1997. Kinematics of the Pacific Equatorial Undercurrent: a Eulerian and Lagrangian approach from GCM results. *J. Phys. Oceanogr.* **27**, 1038–1053.

Döös, K. 1994. Semianalytical simulation of the meridional cells in the Southern Ocean. *J. Phys. Oceanogr.* **24**, 1281–1293.

Döös, K. 1995. Inter-ocean exchange of water masses. *J. Geophys. Res.* **100**, C7, 13 499–13 514.

Döös, K. and Webb, D. J. 1994. The Deacon cell and the other meridional cells in the Southern Ocean. *J. Phys. Oceanogr.* **24**, 429–442.

Fountain, G. O., Khakhar, D. V. and Ottino, J. M. 1998. Visualization of three-dimensional chaos. *Science* **281**, 683–686.

Hirst, A. C., Jackett, D. R. and McDougall, T. J. 1996. The meridional overturning cells of a world ocean model in neutral density coordinates. *J. Phys. Oceanogr.* **26**, 775–791.

Hoppema, M., Fahrbach, E. and de Baar, H. E.W. 2000. Surface layer balance of the Southern Antarctic Circumpolar Current (prime meridian) used to derive carbon and silicate consumptions and annual air–sea exchange for CO_2 and oxygen. *J. Geophys. Res.* **105**, C5, 11 359–11 371.

Lichtenberg, A. J. and Lieberman, M. A. 1983. *Regular and stochastic motion.* Springer-Verlag, New York.

Pierrehumbert, R. T. 1991. Large-scale horizontal mixing in planetary atmospheres. *Phys. Fluids A* **3**, 1250–1260.

Polvani, L. M. and Wisdom, J. 1990. Chaotic Lagrangian trajectories around an elliptic vortex patch embedded in a constant an uniform background shear flow. *Phys. Fluids A* **2**, 123–126.

Webb, D. J. 1996. An ocean model for array processor computers. *Comput. Geosci.* **22**, 569–578.

Webb, D. J. 2000. Evidence for shallow zonal jets in the South Equatorial Current region of the southwest Pacific. *J. Phys. Oceanogr.* **30**, 706–720.